Materials Science-Poland, 35(2), 2017, pp. 283-290
http://www.materialsscience.pwr.wroc.pl/
DOI: 10.1515/msp-2017-0045

DE GRUYTER OPEN

Structural, electronic and magnetic properties of Fe, Co, Ni monatomic nanochains encapsulated in armchair LiF nanotubes

B. ARGHAVANI NIA[1], R. MORADIAN[1,2*], M. SHAHROKHI[3]

[1]Physics Department, Faculty of Science, Razi University, Kermanshah, Iran
[2]Nano-Science and Nano-Technology Research Center, Razi University, Kermanshah, Iran
[3]Young Researchers and Elite Club, Kermanshah Branch, Islamic Azad University, P.O. Box 67149-67346, Kermanshah, Iran

Structural, electronic and magnetic properties of transition metal TM (TM = Fe, Co and Ni) atomic chains wrapped in single walled LiF armchair nanotubes have been investigated by the first-principles calculations in the framework of the density functional theory. The generalized gradient approximation (GGA) with Hubbard repulsion potential and without Hubbard repulsion was employed to describe the exchange-correlation potential. It is found that all these TM chains @LiFNTs systems have negative formation energy so they are stable and exothermic. Total density of states and partial densities of states analyses show that the spin polarization and the magnetic moment of TM chains @LiFNTs(n,n) systems come mostly from the TM atom chains. All these nanocomposites are ferromagnetic (FM) and spin splitting between spin up and down is observed. The high magnetic moment and spin polarization of the TM chains @LiFNT(n,n) systems show that they can be used as magnetic nanostructures possessing potential current and future applications in permanent magnetism, magnetic recording, and spintronics.

Keywords: *LiF nanotube; DFT; encapsulated nanochains; transition metals; Hubbard repulsion*

1. Introduction

Quasi-one-dimensional (1D) nanostructures, such as nanotubes, nanowires and atomic nanochains, have been proved to be promising materials for applications in nanodevices, nanoelectronics, nanolithography, photocatalysis, spintronics and other fields of modern nanotechnologies [1–4]. Transition metal monatomic chains have the ability to be magnetized much more easily than their bulk phase [5, 6], so they are important in the spin-dependent electronic devices, namely, spintronic devices [7]. Due to oxidation it is difficult to fabricate low dimensional homogeneous systems such as ferromagnetic nanowires and nanochains [8]. To avoid this, the electromagnetic nanowires and nanochains are encapsulated inside nanotubes. Fe, Co, Ni and Fe–Ni alloy nanorods/nanowires encapsulated into carbon nanotubes (CNTs) and boron nitride nanotubes (BNNTs) have been fabricated [9–11]. It has been revealed that encapsulated Fe chain in a single walled CNT is more stable than freestanding Fe nanochain [12]. CNTs are totally impermeable to protect electromagnetic nanowires and nanochains from corrosion, and at the same time they are so thin that keep unaltered chemical properties of the protected material. After discovery of carbon nanotubes by Iijima [13] a considerable number of different composite nanoscale tubular structures have been fabricated and investigated, based on crystals, such as SiC [14, 15], BN [16, 17], ZnO [18–23] and BeO [24, 25]. All these nanotubes can be an alternative to carbon nanotubes in encapsulation of electromagnetic nanowires and nanochains. The structural, electronic and magnetic properties of transition metals (TM) nanowires/nanochains encapsulated into

*E-mail: moradian.rostam@gmail.com

BNNTs, BeONTs and ZnONTs have been investigated by first principles study [3, 5, 9, 26–28]. It is found that all those nanocomposites are ferromagnetic (FM) and spin splitting between spin up and down is observed. The structural and electronic properties of the pristine zigzag (n,0) and armchair (n,n) LiFNTs ($3 \leqslant n \leqslant 10$) have been investigated recently [29]. It is found that both zigzag and armchair LiFNTs can exist stably because of their large negative binding energies that are slightly smaller than that of their bulk. Also, density functional theory (DFT) and coupled-cluster (CCSD) calculations have been performed on a series of $(LiF)_{n=2.36}$ neutral clusters by Fernandez Lima et al. [30]. Their results show that nanotube structures with hexagonal and octagonal transversal cross sections show more stability than that of the typical cubic form of large LiF crystals. Furthermore, the insulating character was observed in them [29]. Since the band gap of LiFNTs is larger than in BNNTs, BeONTs and ZnONTs, so the LiFNT is especially suitable for protecting a ferromagnetic nanowire inside its cavity to resist the oxidization of the encapsulated content. Up to now, TM nanochains, such as Fe, Co and Ni encapsulated in the LiFNTs, have not been investigated. In this paper, by density functional theory calculations, we investigated the stable geometries, electronic and magnetic properties of a single TM atomic chain encapsulated in single walled (SW) LiFNTs. The paper is organized as follows: Section 1 is introduction; the computational details are given in Section 2. In Section 3 we presented our calculated results stability, electronic and magnetic properties of pristine SWLiFNTs, freestanding TM chains and TM chains wrapped in the armchair LiFNTs. The last section is conclusions.

2. Computational method

All calculations presented in this work are performed via first principles full potential linearized augmented plane-wave (FP-LAPW) method in the framework of the density function theory (DFT) [31], as implemented in the WIEN2K code [32]. For the exchange-correlation energy functional, we used the generalized gradient approximation (GGA) in the form of Perdew-Burke-Ernzerhof (PBE) [33] with Hubbard repulsion potential and without Hubbard repulsion. The details for the GGA + U can be found in [34, 35]. In GGA + U calculations, we use $U_{effn} = U - J = 2.5$ eV, 1.8 eV, and 2.4 eV for Fe, Co, and Ni [9, 35–37]. In this method, the parameters U and J represent on-site Coulomb interaction energy and exchange energy, respectively. The Brillouin zone integration is performed within the Gamma centered Monkhorst-Pack scheme [38] using $1 \times 1 \times 14$ k-points. The maximum angular momentum of the atomic orbital basis functions is set to $l_{max} = 10$. In order to achieve energy eigenvalues convergence, the wave functionals in the interstitial region are expanded in terms of plane waves with a cut-off parameter of $RMT \cdot K_{max} = 7.5$, where RMT denotes the smallest atomic sphere radius and K_{max} the largest k vector in the plane wave expansion. The Fourier expansion charge density is truncated at $G_{max} = 14$ $Ry^{1/2}$. The Muffin-tin radii are set to RMT = 1.4 a.u. for Li, RMT = 1.6 a.u. for F, RMT = 1.9 a.u. for Fe, RMT = 1.8 a.u. for Co and RMT = 1.7 a.u. for Ni.

3. Result and discussions

3.1. Pristine single-walled LiF nanotubes

To investigate structural and electronic properties of LiFNTs, we choose armchair tubes with four different diameters. The smallest tube studied here is (5,5), and the largest structure is (13,13). All LiFNTs studied here have been fully relaxed to minimize their energies. In relaxation, all atomic positions are relaxed accurately down to the forces of about 1 mRy/a.u. We found Li–F bond length for all different diameters is about 1.79 Å which is in a good agreement with previous results [29]. After relaxation, the anions (F) move slightly outward the tube axis, whereas the cations (Li) move inward with respect to their initial positions; this is due to less atomic radius of fluorine with respect to lithium, hence, higher electronic charge density

of fluorine with respect to lithium atoms. Therefore, the tube surface becomes buckled. After relaxation, the radial geometry of the tubular structure is characterized by two concentric cylindrical tubes, with an outer anionic and an inner cationic cylinders. All the Li atoms form the inner cylinder while all of the F atoms form the outer cylinder. The radial buckling, which indicates the strength of the buckling, is defined by [5, 21]:

$$\beta = r_F - r_{Li} \tag{1}$$

where r_F and r_{Li} are the mean radii of the anion and cation cylinders, respectively. The calculated values of buckling of SWLiFNTs are 0.07 Å, 0.05 Å, 0.035 Å and 0.03 Å for (5,5), (7,7), (11,11) and (13,13) LiFNTs, respectively. Our results are in a very good agreement with previous theoretical data [29]. Obviously, the amount of radial buckling, β, decreases with increasing diameter of LiFNTs. It is predicted that for very large tubes diameters β disappears [29]. This result is similar to the calculated result for SiC, BN, and BeONTs [39]. The radial buckling of LiFNTs is smaller than the corresponding values obtained for SiC, BN, and BeONTs, due to the fact that the Li–F bond length is larger than that of the corresponding NTs. To investigate the electronic properties, we have calculated the density of states (DOS) and electronic band structures for pristine LiFNTs. Fig. 1 shows the band structure along the high symmetry line R-Γ of the 1D NT Brillouin zone and DOS for the (5,5) and (11,11) LiFNTs. The results of Fig. 1 show that the pristine armchair SWLiFNTs have large band gap, which means they are insulators. For all armchair SWLiFNTs, the bottom of the conduction band generally appears at the Γ point of the one-dimensional Brillouin zone, while the top of the valence band occurs at the K point of R-Γ line. It can be seen that the band gap of SWLiFNTs increases with diameter. The calculated energy gaps are 6.5 eV, 6.6 eV, 6.7 eV and 6.72 eV for (5,5), (7,7), (11,11) and (13,13) SWLiFNTs, respectively. Less gap of (5,5) with respect to (13,13) is due to more curvature and hybridization of p orbitals of Li and F. Our results of electronic properties of pristine SWLiFNTs are in a good agreement with previous theoretical results [29].

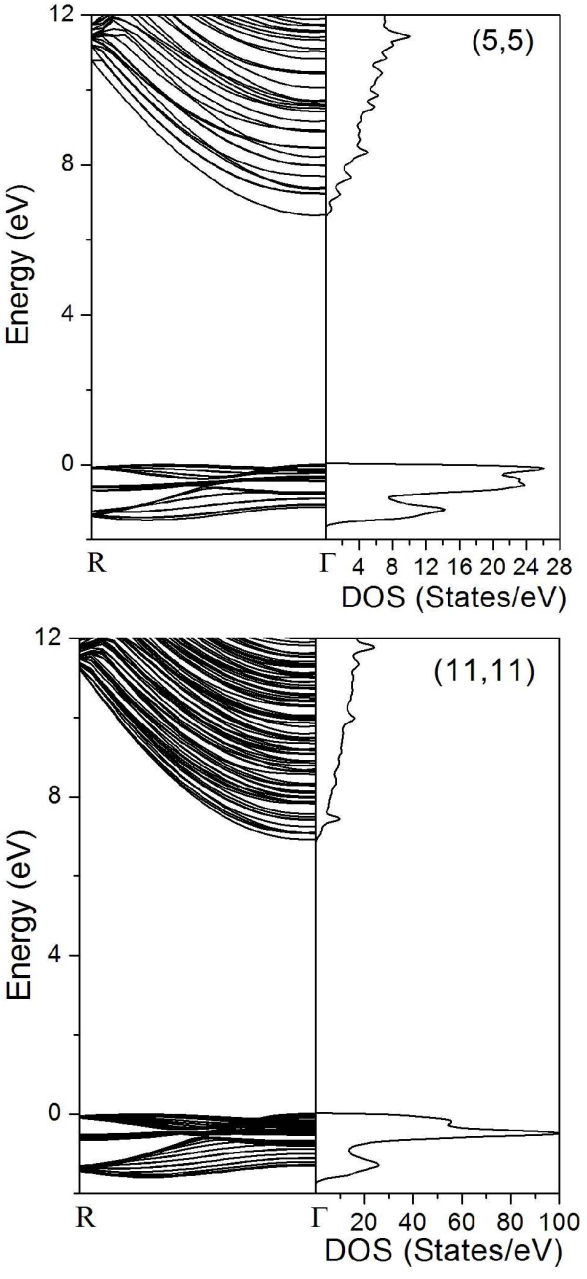

Fig. 1. The electronic band structure along the high symmetry line R-Γ of the 1D NT Brillouin zone and total DOS calculated for pristine (5,5), and (11,11) SWLiFNTs.

3.2. TM nanochains @LiFNTs

3.2.1. Freestanding TM nanochains

In this section, we discuss the structural, electronic and magnetic properties of Fe, Co and Ni linear chains encapsulated in the SWLiFNTs but

Table 1. The calculated values of total magnetic moment per unit cell (in Bohr magnetons μ_B) and the spin polarization for the linear structures of Fe, Co, and Ni nanochains for GGA and GGA + U.

Type	μ		P [%]	
	GGA	GGA + U	GGA	GGA + U
Fe	3.45	3.53	94	82
Co	2.28	2.45	95.5	86
Ni	1.25	1.39	97	92

before encapsulation process we investigate electronic and magnetic properties of freestanding TM nanochains. TM nanochains have linear and planar zig-zag structures [40]. Since linear chains lattice constant just match with the quasi-one-dimensional unit cell length of armchair SWLiFNTs, we considered linear chains encapsulated on armchair LiFNTs. Fig. 2 shows density of states (DOS) for isolated TM linear atomic chains in GGA and GGA + U, respectively. The spin splitting between spin up and down leads to spin polarization which is defined as follows [27]:

$$P = \frac{N_{EF}^{\uparrow} - N_{EF}^{\downarrow}}{N_{EF}^{\uparrow} + N_{EF}^{\downarrow}} \tag{2}$$

where $N_{EF}^{\uparrow}$ and $N_{EF}^{\downarrow}$ represent the density of states of majority spin (spin up) and minority spin (spin down) at the Fermi level, respectively. The magnetization, M, is defined as follows:

$$M = (N^{\uparrow} - N_{\downarrow}) \times \mu_B \tag{3}$$

where $N^{\uparrow}$ and $N_{\downarrow}$ represent the total number of electrons of majority spin and minority spin, respectively. The calculated spin polarization and magnetic moments of Fe, Co and Ni nanochains for GGA and GGA + U are presented in Table 1. The maximum polarization and minimum magnetic moment belong to Ni nanochain while minimum polarization and maximum magnetic moment belong to Fe nanochain. It can be seen that for all TM nanochains, magnetic moments for GGA + U are greater than those found for GGA.

3.2.2. Stability of TM nanochains @LiFNTs

In the next step we calculate electronic and magnetic properties of Fe, Co and Ni chains

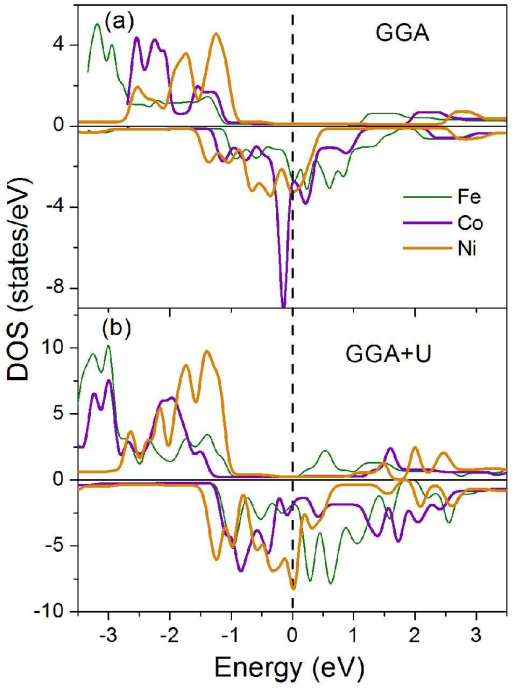

Fig. 2. The majority (up) and minority (down) electrons DOS for isolated Fe, Co and Ni linear atomic chains in GGA and GGA + U.

encapsulated in SWLiFNTs. Theoretical calculations predicted that for carbon and beryllium oxygen nanotubes, when the linear chain is at the nanotube axes, the system in this position is much more stable than in other positions of linear chain deviated from nanotube axes [9, 41]. Furthermore, it has been revealed that TM nanochains encapsulated in single-wall nanotubes are more stable than those in multi-wall nanotubes [9], hence, in present work we only consider TM nanochains encapsulated in single-wall LiFNTs. Fig. 3 shows the structure of (5,5), (7,7), (11,11) and (13,13) SWLiFNTs where encapsulated Fe nanochain is on the nanotubes axes. In order to investigate stability of encapsulated linear TM nanochains inside single walled LiFNTs systems, we have calculated formation energy per unit cell, E_f, for TM@SWLiFNTs system using:

$$E_f = \frac{E_{LiFNT+Chain} - (E_{LiFNT} + E_{Chain})}{n} \tag{4}$$

where $E_{LiFNT+Chain}$, E_{LiFNT} and E_{Chain} are the total energy of TM atomic chains @SWLiFNTs,

pristine LiFNTs and the isolated linear TM atomic chains, respectively. The n is the number of TM atoms per unit cell. For all the systems, the calculations are done for both ferromagnetic (FM) and antiferromagnetic (AFM) cases. We found that all systems in the FM phase are more stable than in AFM case. Calculated values of formation energy for Fe, Co and Ni atomic chains @LiFNTs are listed in Table 2. Our calculated E_f of transition metal chains encapsulated in the LiFNTs systems show that these systems are more stable than individual LiFNTs and TM chain systems. These results show that the interaction between TM chains and LiFNTs is attractive. From Table 2 it is evident that by increasing the diameter of SWLiFNTs, the formation energy of TM@SWLiFNTs moves to the lower energies, hence the larger diameter TM@SWLiFNTs systems are more stable than those with smaller diameters. Our results are in a good agreement with previous results for TM@BeONTs [9]. This can be explained by plotting charge density contour plots. Fig. 4 shows charge density contour plots for Fe chains encapsulated in (5,5) and (11,11) LiFNTs. This figure illustrates that there is a charge transfer from Fe atoms of the chains to F atom and a slight charge transfer from Li atoms to F atoms of LiFNTs. So, the binding between Fe nanochains and LiFNTs has ionic character. By decreasing LiFNTs diameter, the distance between LiFNT and Fe chain is reduced and more electrons transfer from Fe chain to the LiFNTs, hence increasing repulsion between these electrons which leads to increasing the formation energy.

3.2.3. Electronic and magnetic properties of TM nanochains @LiFNTs

To reveal the electrical features of these nanocomposites, the DOS of these systems are calculated. Fig. 5 shows total DOS and atomic partial DOS of TM nanochains encapsulated in the (5,5), (7,7), (11,11) and (13,13)) SWLiFNTs for GGA + U, respectively. Since most transport of electron spin and charge occurs at the Fermi level, we pay more attention on DOS and partial DOS at the Fermi level (vertical dashed line). For all these systems it is found that spin splitting of DOS

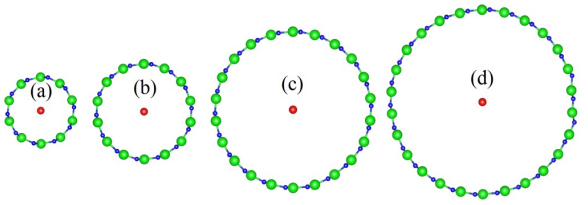

Fig. 3. Cross-sectional views of the optimized structures of Fe linear chain wrapped in (a) (5, 5), (b) (7, 7), (c) (11, 11) and (13, 13) SWLiFNTs. Big green, small blue and medium red balls in the geometrical models represent Li, F and Fe atoms, respectively.

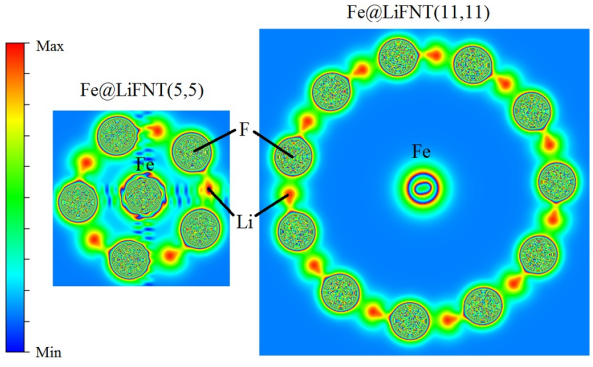

Fig. 4. Contour plots of the charge density distribution on the plane perpendicular to the system axis and through Fe atom located on the axis for (a) Fe@LiFNT(5,5) and (b) Fe@LiFNT(11,11) systems.

around Fermi energy is observed due to strong hybridization of TM 3d orbital with 2s and 2p orbitals of nanotubes atoms. In other words, both the magnetic moment and spin polarization come mostly from TM atoms chain. For energies more than 3 eV and less than –4 eV, the spin splitting disappears and the DOS becomes LiFNTs DOS. The spin splitting leads to spin polarization in all the TM@LiFNTS systems which are shown in Table 2. It is found that by increasing the LiFNT diameter, spin polarization of the nanocomposites is increased for both GGA and GGA + U because for larger diameters the charge transfer from TM nanochain to LiFNT is reduced.

Due to exchange interaction of d orbital electrons, isolated transition metal atoms have a large

Table 2. Calculated values of total magnetic moment μ_{tot} per unit cell (in Bohr magnetons μ_B), partial magnetic moment μ_x per unit cell (in Bohr magnetons μ_B, x = Fe, Co and Ni), formation energy E_f (in eV) and spin polarization for Fe, Co and Ni monoatomic chains @LiFNTs (the values inside the parenthesis belong to GGA + U).

Type	μ_{tot}	μ_x	E_f	Polarization [%]
Fe@(5,5)	3.4 (3.45)	2.98 (2.97)	–2.12 (–1.9)	83 (71)
Fe@(7,7)	3.41 (3.47)	3.14 (3.25)	–2.33 (–2.00)	85 (74)
Fe@(11,11)	3.45 (3.53)	3.18 (3.27)	–2.7 (–2.44)	90 (80)
Fe@(13,13)	3.46 (3.53)	3.2 (3.29)	–2.82 (–2.50)	92.5 (82)
Co@(5,5)	2.20 (2.41)	2.17 (2.20)	–1.30 (–1.10)	86 (74)
Co@(7,7)	2.22 (2.41)	2.20 (2.23)	–1.54 (–1.25)	88 (78)
Co@(11,11)	2.28 (2.45)	2.22 (2.25)	–1.88 (–1.65)	94 (85)
Co@(13,13)	2.29 (2.46)	2.22 (2.28)	–1.97 (–1.70)	95.5 (86)
Ni@(5,5)	1.19 (1.27)	1.15 (1.23)	–1.17 (–0.91)	88 (78)
Ni@(7,7)	1.20 (1.32)	1.15 (1.24)	–1.25 (–0.95)	90 (80)
Ni@(11,11)	1.23 (1.36)	1.18 (1.26)	–1.74 (–1.44)	96 (90)
Ni@(13,13)	1.25 (1.38)	1.20 (1.27)	–1.81 (–1.50)	97.3 (93)

magnetic moment but when these atoms create a crystal, some of electrons are bounded to other atoms, hence, the magnetic moment is reduced. Furthermore, LiFNTs has non-magnetic structure, but it may have magnetic properties by encapsulating the magnetic nanochains. Our calculated results of magnetic moment per unit cell and partial atomic transition metal magnetic moment for isolated Fe, Co and Ni nanochains @LiFNTs are presented in Table 2. It can be seen from this table that in TM@SWLiFNTs both magnetic moment and spin polarization increase by increasing the tube diameter but they do not exceed those of individual TM atoms chain. For all these systems, total and partial magnetic moments are reduced with respect to isolated TM chains what is due to hybridization of 3d orbital of TM chains with 2s and 2p orbitals of LiFNTs. The magnetic moments for larger diameters are equal to the magnetic moments of individual TM chains due to weak hybridization between TM chains and LiFNTs. For example, the magnetic moment of TM atoms of TM chains @LiFNT(13,13) system attains the maximum compared with those for other TM chains @LiFNTs (n,n) systems. Magnetic moment of Fe chain @LiFNTs is much larger than that of Co and Ni chains @LiFNTs. Also for all TM nanochains @LiFNTs, magnetic moments for GGA + U are greater than those found for GGA.

To get more insight about the effects of TM encapsulation on electronic properties of LiFNTs, the orbital partial DOS (PDOS) have been calculated from the GGA + U for individual LiFNTs and Fe@LiFNTs and the obtained results have been compared. The GGA + U partial electronic DOS of (5,5) and (13,13) LiFNTs before and after Fe chain encapsulation are shown in Fig. 6. As can be seen from Fig. 6, the Fe chain encapsulation has led to a constant shift of the pristine LiFNT bands, where both occupied and unoccupied bands are moved to lower energies. Furthermore, it creates some spin polarized states in the band gap of pristine LiFNTs. These changes for Fe@(5,5)LiFNT are more remarkable than for Fe@(13,13)LiFNT because of strong hybridization between Fe chain and LiFNTs with smaller diameters.

4. Conclusions

In this paper, for the first time, we have reported first-principles calculations details of structural, electronic and magnetic properties of the Fe, Co and Ni atomic chains wrapped in the single walled armchair LiFNTs. First of all, by comparing the structural properties of individual SWLiFNTs, we have found that due to higher electronic charge density of fluorine with respect to lithium atoms the tube surface of LiFNTs becomes buckled. After relaxation, the anions (F) move slightly outward with respect to the tube axis, whereas the cations (Li) move inward with respect to their initial positions. Electronic band structures and total DOS

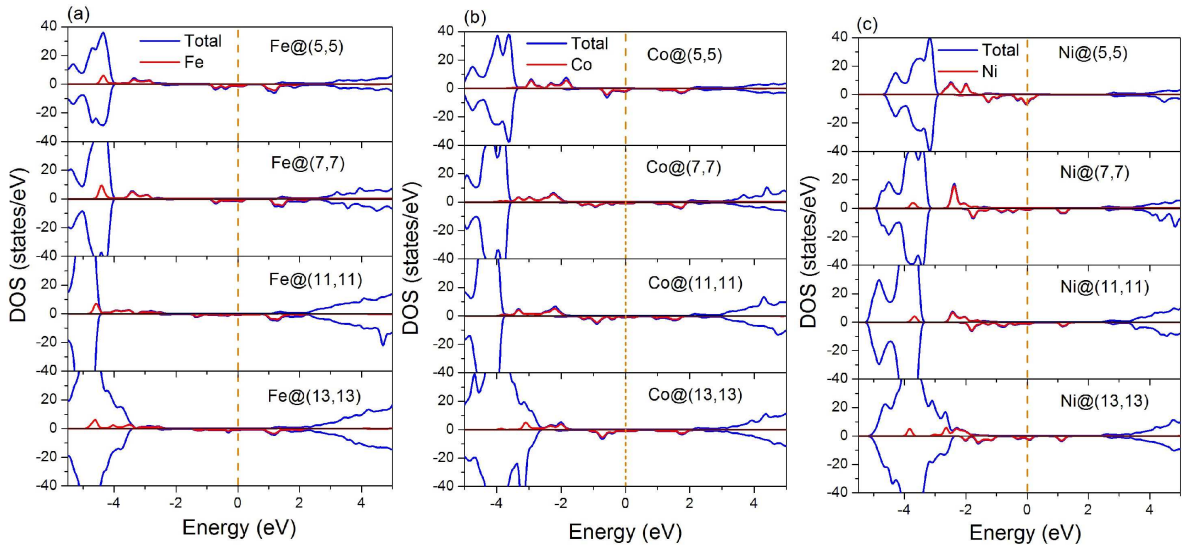

Fig. 5. Total and partial DOS for (a) Fe, (b) Co and (c) Ni atomic chains @LiFNTs using GGA + U, respectively. The Fermi energy is aligned to zero.

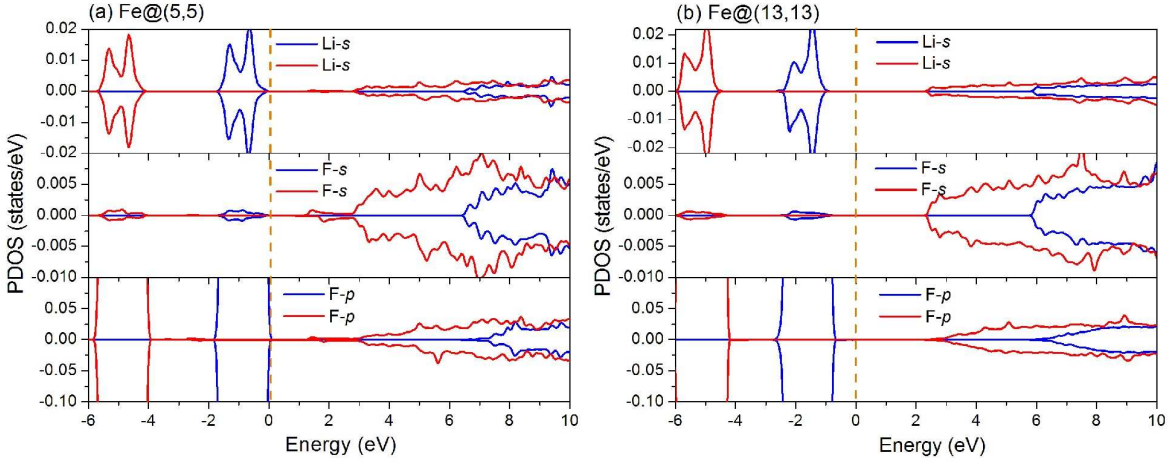

Fig. 6. The orbital partial DOS calculated for (5,5), and (13,13) SWLiFNTs before (blue line) and after (red line) Fe chain encapsulation using GGA + U. The Fermi energy is aligned to zero.

of these systems show that the individual armchair SWLiFNTs have large indirect band gap (about 6.5 eV), which means that they are insulators while the total density of states of TM chains @LiFNTs reveals their half metallic character with spin polarization and a net magnetic moment. Calculated formation energies for all TM chains @LiFNTs systems are negative which implies that formation processes of these systems are exothermic. The larger diameter TM@SWLiFNTs systems are more stable than the ones with smaller diameters because by decreasing LiFNTs diameter the distance between LiFNT and Fe chain is reduced and more electrons transfer from Fe chain to the LiFNTs, hence increasing repulsion between these electrons which leads to increasing formation energy. It is found that in TM@SWLiFNTs by increasing nanotubes diameter, the formation energy is decreased while local magnetic moments, total magnetic moments and spin polarization are increased. For all TM atomic chains @LiFNTs with smaller diameters the magnetic moment is strongly reduced with

respect to individual chains which is due to hybridization of 3d orbital of transition metal chains with 2s and 2p orbitals of LiFNTs. Our results show that the electronic and magnetic properties of these nanocomposites are similar to TM@BeONTs [9], however, they are less stable than TM@BeONTs.

References

[1] LI H., ZHAO N., HE C., SHI C., DU X., LI J., *J. Alloy. Compd.*, 465 (2008), 51.

[2] IVANOVSKAYA V.V., KÖHLER C., SEIFERT G., *Phys. Rev. B*, 75 (2007), 075410.

[3] SHAHROKHI M., MORADIAN R., *Eur. Phys. J. Appl. Phys.*, 65 (2014), 20402.

[4] SHAHROKHI M., NADERI S., FATHALIAN A., *Solid State Commun.*, 152 (2012), 1012.

[5] NADERI S., SHAHROKHI M., NORUZI H.R., GURABI A., MORADIAN R., *Eur. Phys. J. Appl. Phys.*, 62 (2013), 30402.

[6] DELIN A., TOSATTI E., *Phys. Rev. B*, 68 (2003), 144434.

[7] WOLF S.A., AWSCHALOM D.D., BUHRMAN R.A., DAUGHTON J.M., MOLNÁR S., ROUKES M.L., CHTCHELKANOVA A.Y., TREGER D.M., *Science*, 294 (2001), 1488.

[8] HAMADA N., SAWADA S.I, OSHIYAMA A., *Phys. Rev. Lett.*, 68 (1992), 1579.

[9] MORADIAN R., SHAHROKHI M., MORADIAN S., *Physica E*, 47 (2013), 40.

[10] GOLBERG D., XU F.F,. BANDO Y., *Appl. Phys. A*, 76 (2003), 479.

[11] TANG C., BANDO Y., GOLBERG D., DING X., QI SH., *J. Phys. Chem. B*, 107 (2003), 6539.

[12] FAGAN S.B., MOTA R., ANTÔNIO J.R.S., FAZZIO A., *Microelectron. J.*, 34 (2003), 481.

[13] IIJIMA S., *Nature*, 354 (1991), 56.

[14] SUN X.H., LI C.P., WONG W.K., WONG N.B., LEE C.S., LEE S.T., TEO B.K., *J. Am. Chem. Soc.*, 124 (2002), 14464.

[15] BEHZAD S., CHEGEL R., MORADIAN R., SHAHROKHI M., *Superlattice. Microst.*, 73 (2014), 185.

[16] LEE R.S., GAVILLET J., LAMY DE LA CHAPELLE M., LOISEAU A., COCHON J.L., PIGACHE D., THIBAULT J., WILLAIME F., *Phys. Rev. B*, 64 (2001), 121405.

[17] MORADIAN R., SHAHROKHI M., CHARGANEH S.S., MORADIAN S., *Physica E*, 46 (2012), 182.

[18] XING Y.J., XI Z.H., ZHANG X.D., SONG J.H., WANG R.M., XU J., XUE Z.Q., YU D.P., *Solid State Commun.*, 129 (2004), 671.

[19] MORADIAN R., SHAHROKHI M., *Physica E*, 44 (2012), 1760.

[20] MORADIAN R., SHAHROKHI M., *J. Phys. Chem. Solids*, 74 (2013), 1063.

[21] SHAHROKHI M., MORADIAN R., *Indian. J. Phys.*, 89 (2014), 249.

[22] ESMAILIAN A., SHAHROKHI M., KANJOURI F., *Int. J. Mod. Phys. C*, 26 (2015), 1550130.

[23] ARGHAVANI NIA B., SHAHROKHI M., MORADIAN R., MANOUCHEHRI I., *Eur. Phys. J. Appl. Phys.*, 67 (2014), 20403.

[24] FATHALIAN A., MORADIAN R., SHAHROKHI M., *Solid State Commun.*, 156 (2013), 1.

[25] SHAHROKHI M., LEONARD C., *J. Alloy. Compd.*, 682 (2016), 254.

[26] YANG C.K., ZHAO J., PING LU J., *Phys. Rev. B*, 74 (2006), 235445.

[27] MORADIAN R., SHAHROKHI M., KARAMI POURIAN A., *J. Magn. Magn. Mater.*, 344 (2013), 162.

[28] MORADIAN R., SHAHROKHI M., AMJAIAN S., SAMADI J., IJADI R., *Eur. Phys. J. Appl. Phys.*, 67 (2014), 20406.

[29] WANG S.F., CHEN LI Y., ZHANG Y., ZHANG J.M., JI V., XU K.W., *J. Phys. Chem. C*, 116 (2012), 1657.

[30] FERNANDEZ LIMA F.A., HENKES A.V., SILVEIRA E.F., MARCO A.C.N., *J. Phys. Chem. C*, 116 (2012), 4969.

[31] BLAHA P., SINGH D.J., SORANTIN P.I., SCHWARZ K., *Phys. Rev. B*, 46 (1992), 1325.

[32] BLAHA P., SCHWARZ K., MADSEN G.K.H., LUITZ J., WIEN2k: *An Augmented Plane Wave plus Local Orbitals Program for Calculating Crystal Properties*, 2001.

[33] PERDEW J.P., BURKE K., ERNZERHOF M., *Phys. Rev. Lett.*, 77 (1996), 3865.

[34] ANISIMOV V.I., SOLOVYEV I.V., KOROTIN M.A., CZYŻYK M.T., SAWATZKY G.A., *Phys. Rev. B*, 48 (1993), 16929.

[35] LIECHTENSTEIN A.I., ANISIMOV V.I., ZAANEN J., *Phys. Rev. B*, 52 (1995), 5467.

[36] LANY S., RAEBIGER H., ZUNGER A., *Phys. Rev. B*, 77 (2008), (24) 241201.

[37] SHOAIB MOHAMMED Y., YU Y., HONGXIA W., KAI L., XIAOBO D., *J. Magn. Magn. Mater.*, 322 (2010), 653.

[38] MONKHORST H.J., PACK J.D., *Phys. Rev. B*, 13 (1976), 5188.

[39] BAUMEIER B., KRÜGER P., POLLMANN J., *Phys. Rev. B*, 76 (2007), 085407.

[40] ATACA C., CAHANGIROV S., DURGUN E., JANG Y.R., CIRACI S., *Phys. Rev. B*, 77 (2008), 214413.

[41] WANG S.F., CHEN LI Y., ZHANG Y., ZHANG J.M., XU K.W., *J. Mol. Struc. THEOCHEM.*, 962 (2010), 108.

Received 2016-06-08
Accepted 2017-03-18